Available online at www.sciencedirect.com
ScienceDirect
Ceramics International 36 (2010) 1265–1275
CERAMICS INTERNATIONAL
www.elsevier.com/locate/ceramint

The effect of pre-milling/pre-synthesis process and excess Ba on the microstructure and dielectric/piezoelectric properties of nano-sized $0.94[(Bi_{0.5}Na_{0.5})TiO_3]–0.06[Ba_{(1+x)}TiO_3]$

Man-Soon Yoon, Neamul Hayet Khansur, Soon-Chul Ur *

Department of Materials Science and Engineering, Research Center for Sustainable Eco-Devices and Materials (ReSEM), Chungju National University, Chungbuk 380-702, Republic of Korea

Received 16 October 2009; received in revised form 2 December 2009; accepted 19 December 2009
Available online 28 January 2010

Abstract

Lead-free piezoelectric ceramic specimens of $0.94[(Bi_{0.5}Na_{0.5})TiO_3]–0.06[Ba_{(1+x)}TiO_3]$ (where $0 \leq x \leq 0.03$) (abbreviated as nano-sized BNBT6(x)) compositions containing excess Ba were synthesized by a modified mixed oxide method. In this modified process $(Bi_{0.5}Na_{0.5})TiO_3$ and $Ba_{(1+x)}TiO_3$ were separately prepared by pre-milling the starting powders in high energy mill (HEM) in order to obtain nano-particle size. BNBT6(x) specimens were also prepared by the conventional process to be compared with the former one. The pre-milling of the raw materials lowered the calcination temperatures of $(Bi_{0.5}Na_{0.5})TiO_3$ and $Ba_{(1+x)}TiO_3$ by 110 and 200 °C, respectively, as compared with the conventional process. High energy milling improved the reaction activity and homogeneity of the materials used throughout the process, enhanced the sintering density and grain uniformity, and decreased the grain size. The effects of excess Ba on the characteristic of nano-sized BNBT6(x) specimens were systematically investigated. The piezoelectric and dielectric properties of BNBT6(x) specimens containing various amounts of excess Ba show maximum values of the planar electromechanical coupling factor (k_p) of 38% and the piezoelectric constant (d_{33}) of 198 pC/N with Ba excess amount of 0.02 mol [BNBT6(0.02)]. The d_{33} then decreases with increasing excess Ba content to 0.03 mol, whereas the relative dielectric permittivity (K^T_{33}) steadily increases with increasing excess Ba and reaches the maximum value of 785 for this composition. Besides, the depolarization temperature (T_d) slightly decreased within the range of $x = 0$–0.01 mol and then tends to rapidly decrease with the excess Ba of 0.02 mol. In addition to this, the T_d remains unchanged with the higher excess Ba of 0.03 mol. The modified mixing and milling method were considered to be a new and promising process for lead-free piezoelectric ceramics owing to their excellent piezoelectric/dielectric properties.

Keywords: Piezoelectric; Pre-milling and Pre-synthesis; Nano-sized BNBT; Excess Ba

1. Introduction

Lead-free piezoceramics have received considerable attention because the lead oxide (PbO) in lead piezoelectric ceramics is volatile and detrimental to human health and the environment; moreover the volatilization of PbO during sintering also generates instability in the composition and the electrical properties of the products. Recently emerged environmental issues will prohibit us from using lead based materials in the near future due to their toxicity. In an approach to acclimate ourselves to recent ecological consciousness trend [1,2], a lead-free piezoelectric material, bismuth sodium barium titanate, was considered as an environment-friendly alternative for a lead based piezoelectric system.

Bismuth sodium titanate, $Bi_{0.5}Na_{0.5}TiO_3$ (BNT), is a kind of $[ABO_3]$-type perovskite ferroelectrics discovered in 1960 [3]. It is considered to be an excellent candidate as a key material for lead-free piezoelectric ceramics because of its strong ferroelectricity and large remnant polarization [3]. The dielectric properties of BNT also showed an interesting anomaly wherein a low temperature phase transition at 200 °C marked the transition from ferroelectric to antiferroelectric [4]. However, because of its high coercive field, $E_c = 73$ kV/cm with relatively large conductivity, pure BNT is difficult to pole and cannot be a good piezoelectric material. To address this problem, many derivatives of BNT-based solid solutions have been developed

* Corresponding author.
E-mail address: scur@cjnu.ac.kr (S.-C. Ur).

0272-8842/$36.00
doi:10.1016/j.ceramint.2010.01.011

[5–9]. Among them, the $(Na_{0.5}Bi_{0.5})_{1-x}Ba_xTiO_3$ (NBT–BT) system has been paid considerable attention on account of the existence of a rhombohedral–tetragonal morphotropic phase boundary (MPB) near $x = 0.06$. Compared with pure NBT, the NBT–BT compositions near the MPB show a considerable decrease in E_c and substantial improvement in piezoelectric properties [6]. Extensive research is going on to further improve the electrical properties of the BNT–BT system by means of microstructural or compositional modifications [10–12]. It was believed that substitution at A-site or B-site might induce soft or hard properties in a piezoelectric material by forming cation or oxygen vacancies, respectively. Several kinds of cations such as La^{3+}, Nb^{5+}, Co^{3+} and Mn^{2+} were tested to modify BNT-based piezoelectrics [13–16].

In BNT system, Bi which is the main contributor for its superior ferroelectric property [17,18], is a volatile constituent at high temperatures, causing compositional deviation from stoichiometry. It has been reported that Bi deficiency increase the leakage current in BNT during the poling process and decrease the piezoelectric properties [19]. Thus, to effectively avoid Bi deficiency, low temperature sintering and/or adding excess Bi into BNT is a prospective method for compositional compensation.

It is well known that the addition of $BaTiO_3$ into the BNT system decreases the E_c. It was reported that the E_c of BNT is influenced by Bi^{3+} ions, i.e., E_c becomes higher with the increasing amount of Bi^{3+} ions, making difficult to pole and leading to low K^T_{33} as a consequence [20]. However, during the traditional process for fine $BaTiO_3$ powders synthesis via a solid-state reaction between titanium oxide and barium carbonate, the barium ion is prone to dissolve in the aqueous system. As a consequence, Ba deficiency is unavoidable in the composition. Because of the vaporization of Bi ions and the dissolution of Ba ions, it is important to control the compositional deviation from stoichiometry. In view of the facts discussed above, one can expect that lowering the sintering temperature and adding the properly designed excess Ba may avoid the compositional deviation and increase the piezoelectric properties of BNBT.

The main purpose of the present study is to control the size and morphology of starting powder in order to increase the reaction activity using a high energy mill (HEM). Furthermore, BNT and $Ba_{(1+x)}TiO_3$ are separately prepared and then mixed to synthesize BNBT ceramics in order to systematically investigate the effect of excess Ba on the microstructure and piezoelectric properties near the MPB region. The effect of

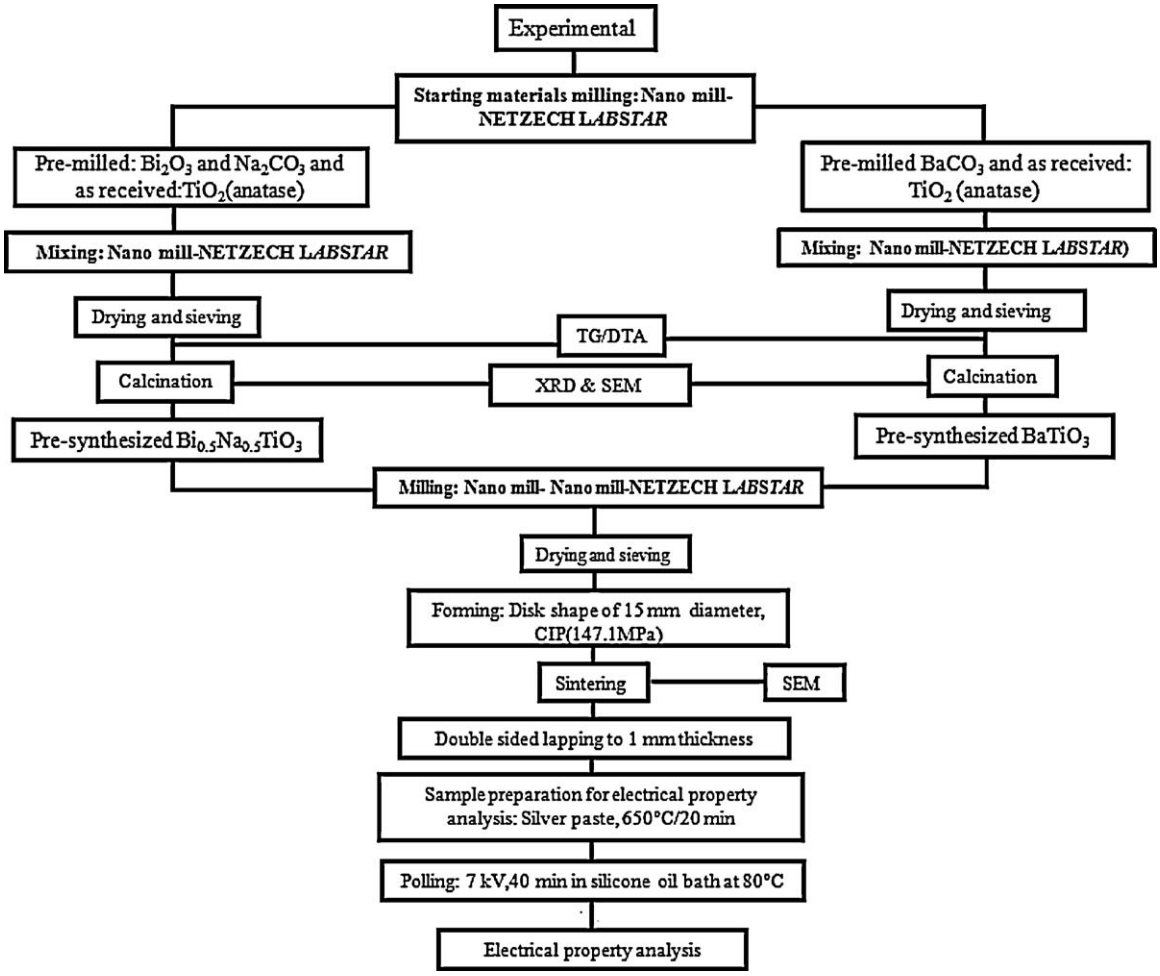

Fig. 1. Processing flow diagram for BNBT preparation.

excess Ba on the depolarization temperature has also been investigated.

2. Experimental procedure

A modified mixed oxide method has been used to fabricate $0.94[(Bi_{0.5}Na_{0.5})TiO_3]$–$0.06[Ba_{(1+x)}TiO_3]$ ($x = 0$, 0.01, 0.02 and 0.03) (abbreviated as nano-sized BNBT6(x)) specimens. In this process $(Bi_{0.5}Na_{0.5})TiO_3$ (abbreviated as nano-sized BNT) and $Ba_{(1+x)}TiO_3$ (abbreviated as nano-sized BT(x)) were separately prepared by pre-milling the starting powders in a HEM (NETZECH L*ABSTAR*). These pre-synthesized BNT and BT were mixed according to the designated composition of BNBT. All the mixing and milling was done in a HEM. The detailed fabrication flow diagram is shown in Fig. 1. Pre-milling of all of the starting materials was conducted in ethanol (99.9%) with mixed sized zirconium beads (diameter of 0.1 and 0.3 mm) and rotor speed of 3000 rpm for 1 h.

Stoichiometric amount of the pre-milled Bi_2O_3, Na_2CO_3 and as-received anatase phase TiO_2 with 100 nm size were mixed in ethanol (99.9%) using HEM with rotor speed of 3000 rpm for 1 h to fabricate nano-sized BNT. The BNT powders were calcined at 650 °C for 3 h. The nano-sized BT(x) powders were also prepared from the corresponding pre-milled starting materials under the same conditions, except different calcination temperature of 950 °C for 2 h. Calcination powders of

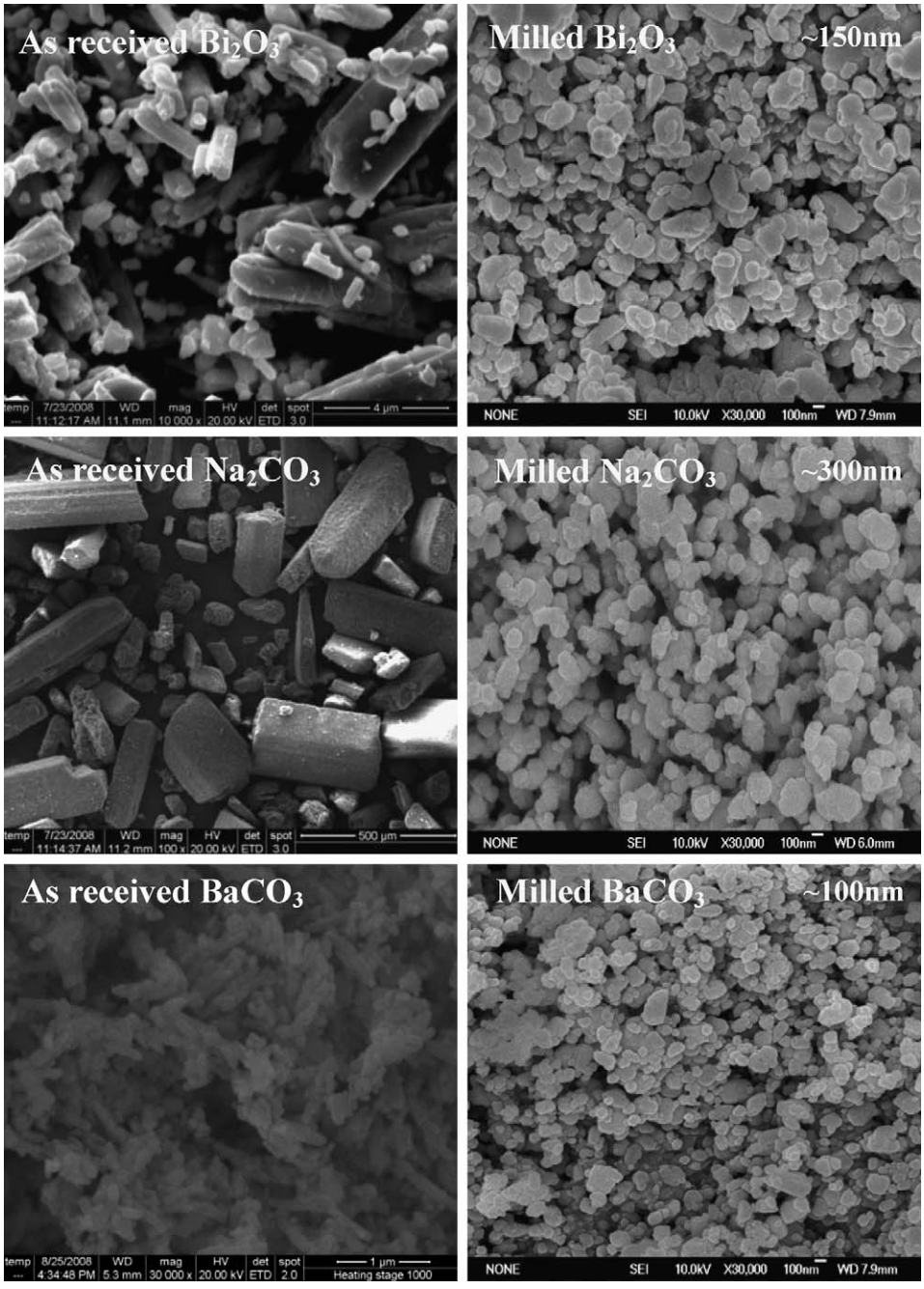

Fig. 2. SEM morphology of the as received and high energy milled starting materials.

BT(x) were analyzed by the inductively coupled plasma spectroscopy (ICP) to confirm the variation of Ba/Ti ratio possibly due to the dissolution of Ba ion. BNT and BT(0) powders were also prepared by using a conventional ball-mill. The calcination temperatures used for conventional BNT and BT(0) were 760 and 1150 °C for 4 h, respectively.

The last step was the synthesis of BNBT6(x). In order to obtain nano-sized particles, the pre-synthesized BNT and BT(x) were mixed and milled using the HEM. Without calcination step, the dried powders were directly pressed. The pressed samples were then sintered at 1140 °C for 2 h. For the purpose of comparing the proposed process with conventional process, BNBT(0) specimens were also prepared with conventional mixing and milling method using a ball mill.

The phase-formation characteristics and tetragonality for the sintered BNBT6(x) were determined using X-ray diffraction (XRD) analysis. The powder morphologies and microstructures were investigated using scanning electron microscopes (SEM, JEOL JSM-6700F and FEI Company Quanta400). In order to measure the electrical properties, silver paste was coated to form electrodes on both sides of the sample, and then subsequently fired at 650 °C for 20 min. The dielectric and the piezoelectric properties were measured using an impedance/gain phase analyzer (HP-4194A) after poling under 7.5 kV/mm at 80 °C in a silicone oil bath for 40 min. Piezoelectric properties were calculated from resonance/anti-resonance measurement method [21]. Temperature dependence of the dielectric constant and dissipation factor over the range from room temperature to 350 °C was measured using an automated system at 1 kHz, whereby HP-4194A and a temperature-control box (Lindberg tube furnace) were controlled by a computer system. To obtain P–E hysteresis curve, the induced electric polarization was measured using a Precision LC system (Radiant Technology Model: 610E).

3. Results and discussion

3.1. Effects of pre-milled starting powders on the reaction temperature and powder morphology of BNT and BT

In order to investigate the effect of pre-milling process of the starting powders on the reaction temperature and powder morphology of BNT and BT(0), the starting powders except TiO_2 (sphere particle morphology with average size of 100 nm) were milled using the HEM. Fig. 2 shows the SEM micrographs of as-received and pre-milled Bi_2O_3, Na_2CO_3 and $BaCO_3$. It can be seen that the process causes a significant change in particle morphology, accompanying the powder shape change from a squared rod shape to sphere shape with average particle size of 150, 300 and 100 nm for Bi_2O_3, Na_2CO_3 and $BaCO_3$, respectively.

Figs. 3(a) and (b) show SEM morphologies of the calcined powders of the nano-milled and conventionally ball-milled BNT. It can be seen that nano-sized BNT having fine and sphere shaped particle morphology compared to the conventional one, which has large and irregular particle distribution. Fig. 3(c) shows the X-ray diffraction patterns for the calcined BNT samples fabricated by the pre-milling process and conventional process. All of them are fully stabilized to perovskite structure without second and/or pyrochlore phases. Especially, despite of low calcination temperature, second and/or pyrochlore phases did not exist in the pre-milled BNT. Thermogravimetric behaviors indicate that the pre-milling process of starting materials is effective in decreasing the reaction temperature by

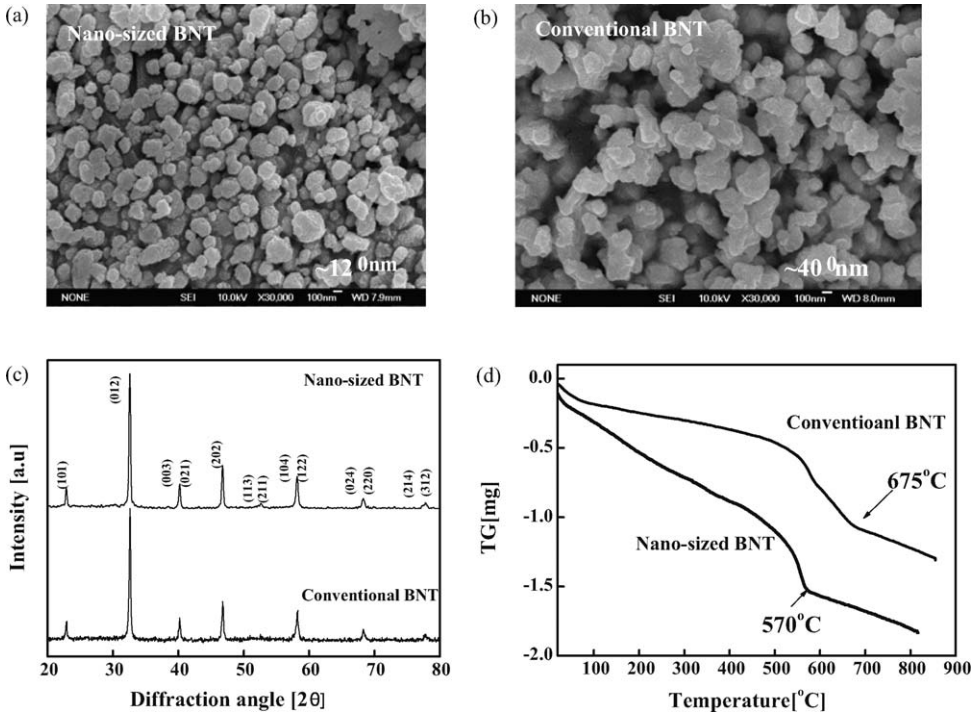

Fig. 3. SEM morphology, XRD patterns and thermogravimetric (TG) behavior of nano-sized BNT fabricated by pre-milled Bi_2O_3, $NaCO_3$ and conventional BNT.

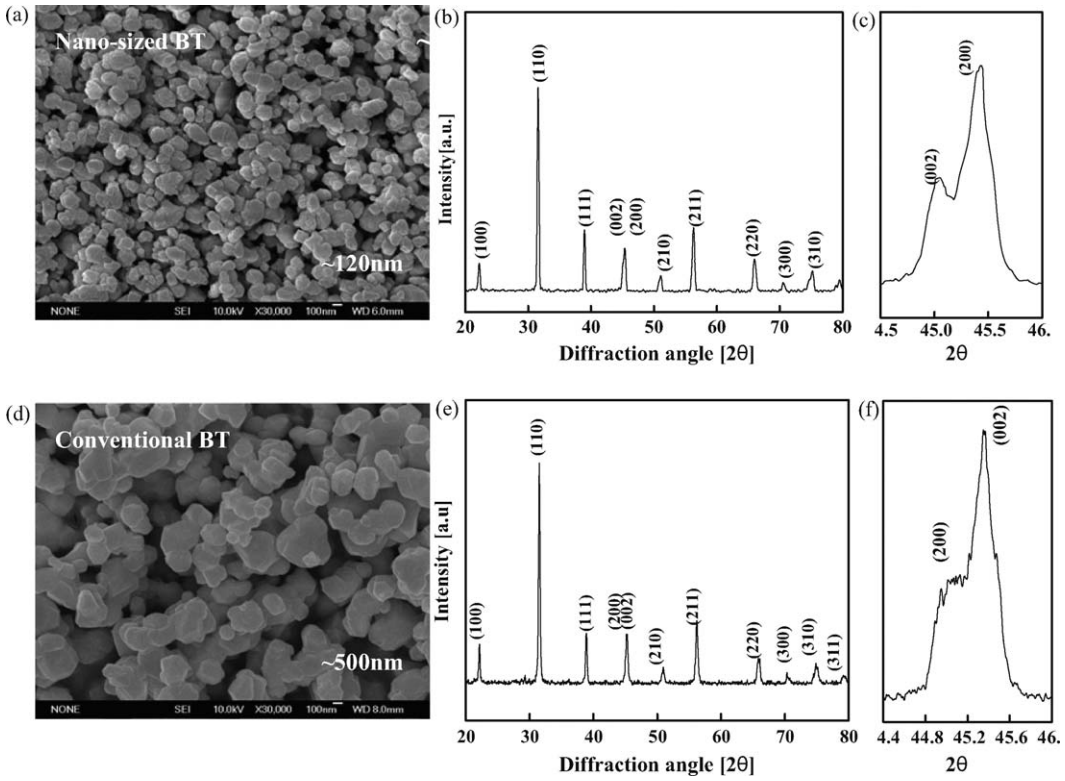

Fig. 4. The powder morphology and X-ray diffraction patterns: (a)–(c), SEM micrograph, X-ray diffraction patterns and (2 0 0) reflection of $BaTiO_3$ fabricated by pre-milled $BaCO_3$ and (d)–(f), SEM micrograph, X-ray diffraction patterns and (2 0 0) reflection of conventional $BaTiO_3$.

almost 110 °C compared to that of the conventionally prepared BNT powder as shown in Fig. 3(d). In addition to these results, weight loss due to carbonate removal is advanced in pre-milled BNT powder, suggesting the increase in surface area and activity.

The high reaction temperature of $BaTiO_3$ will be expected to retard the reaction of BNBT [22,23]. Moreover, since the powder prepared from conventional method had been known to result in a significant amount of agglomeration and poor chemical homogeneity along with a coarse particle size due to the treatment at high temperature. The additionally adopted pre-milling process of $BaCO_3$ was performed to ensure the fine particle size and decrease the reaction temperature. The powder morphology and X-ray diffraction patterns of nano-sized BT and conventional BT were observed as shown in Fig. 4. The average particle size of nano-sized BT was 120 nm, showing the sphere and regular shape, whereas conventional BT having irregular shape with 500 nm particle size. These results are basically consistent with those of previous work [24]. Nano-sized BT was also fully stabilized to perovskite structure despite of low calcination temperature. In addition to this, (2 0 0) and (0 0 2) peaks were separated more obvious than those of conventional BT.

Table 1
Analyzed ICP results for various Ba/Ti ratios.

$BaCO_3$:TiO_2 (mixing ratio)	Results of ICP analysis (Ba/Ti mole ratio)
1:1	0.988142
1.01:1	0.999900
1.02:1	1.001100
1.03:1	1.002300

ICP analysis was performed to observe the variation of Ba/Ti mole ratio in the nano-sized BT(x) as a function of mixing ratio, as presented in Table 1. It can be seen that the dissolution of Ba ion occurs and this in turn denotes that the stoichiometric composition of $Ba_{(1+x)}TiO_3$ appears between BT(0) and BT(0.01).

Fig. 5 shows the TG/DTA analysis results of BNBT6(0) powders, fabricated by two different processes. The weight loss of the conventionally prepared BNBT6(0) is attributed to the decomposition of carbonate. In addition to weight loss, the solid reaction peak caused by the formation of the perovskite solid solution also appears around 850 °C as shown in Fig. 5(a). On the other hand, the weight loss and the solid solution reaction peaks of BNBT6(0) for the nano-sized BNT6(0) mixed with the nano-sized BT(0) was absent since BNT and BT are separately pre-synthesized as shown in Fig. 5(b). The TG/DTA results of nano-sized BNBT6(0) indicate that additional calcination process can be eliminated before the sintering in case of using the pre-synthesized BNT6 and BT(0).

Fig. 6 shows the SEM morphology of the nano-milled BNBT6(0) and conventional ball-milled BNBT6(0) powders. Since the high energy pre-milling processes induced a fine particle size and weakened neck growth due to the lowering calcination temperature of BNT and BT(0) as shown in Figs. 3(a) and 4(a), the particle size of the BNBT6(0) powder after high energy milling was reduced to 90 nm, whereas that of the conventionally ball-milled powders without pre-milling and pre-synthesis has a large and irregular particle size above

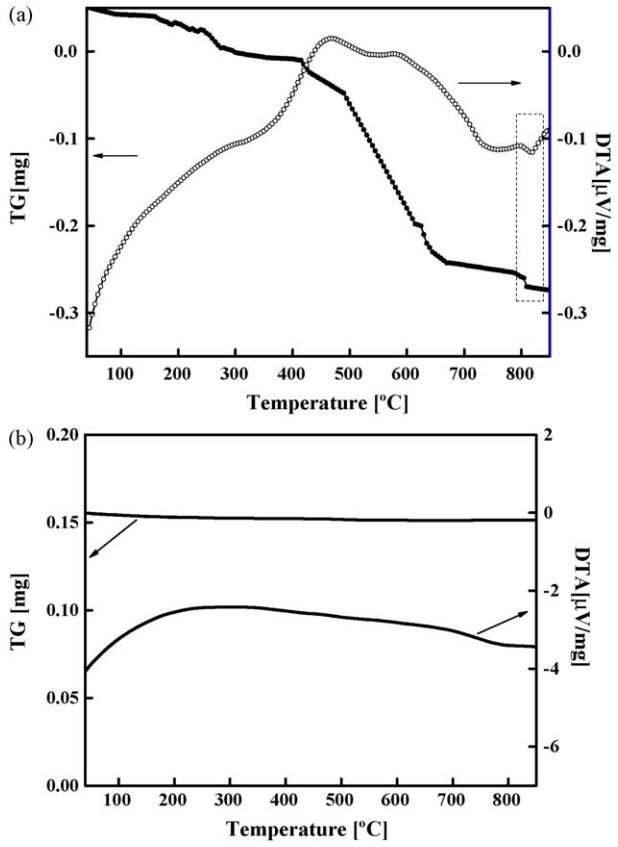

Fig. 5. Comparison of the solid-state reaction temperature using TG/DTA results among different process in air with heating rate of 3 °C/min: (a) conventional BNBT6(0) and (b) nano-sized BNBT6(0) fabricated by using pre-milling and pre-synthesis processes.

300 nm. Therefore, it is expected that homogenously mixed nano-powders enhance the solid–solid reaction with good sinterability due to their higher activity.

3.2. Effects of the excess Barium on crystal structure and microstructure

The XRD patterns of sintered BNBT6(x) compositions sintered at 1140 °C are presented in Fig. 7. A full stabilization of

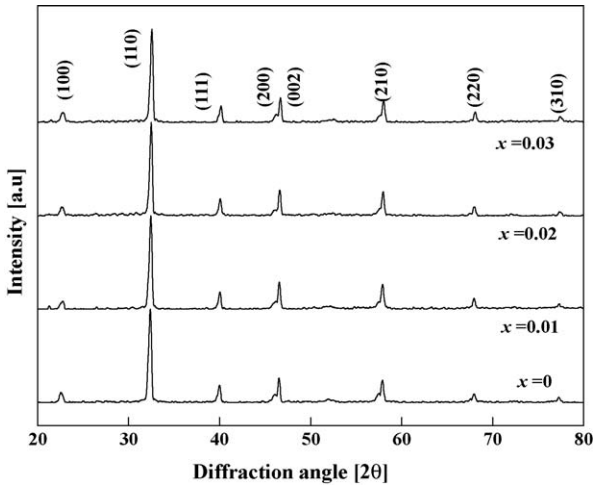

Fig. 7. X-ray diffraction patterns of BNBT6(x) specimens sintered at 1140 °C as a function of excess amounts of Ba.

perovskite phase was achieved for the whole range of compositions. Further XRD analysis was performed in the 2θ ranges of 38–42° and 44–48° as in Fig. 8. Splitting of XRD peaks was detected for all of the specimens, which can be roughly assigned to a (0 0 3)/(0 2 1) and a (0 0 2)/(2 0 0) peak splitting according to a rhombohedral symmetry and a tetragonal symmetry, respectively [6]. This in turn means that all samples of $0.94[(Bi_{0.5}Na_{0.5})TiO_3]$–$0.06[Ba_{(1+x)}TiO_3]$ compositions show the coexistence of tetragonal and rhombohedral symmetry which is consistent with the nature of the specimens with MPB composition [25,26]. As shown in Fig. 8(a), the (0 0 3)/(0 2 1) peak splitting become more distinguishable up to the excess Ba = 0.02 mol. In addition to this, a distinct peak separation can be seen at same composition as shown in Fig. 8(b). It seems that the MPB composition is in the vicinity of BNBT6(0.02), i.e., $0.94[(Bi_{0.5}Na_{0.5})TiO_3]$–$0.06[Ba_{(1+0.02)}TiO_3]$.

To observe the effect of excess Ba on the tetragonality, multiple peak separation method was used for the estimation of c/a as shown in Fig. 9. The ratio of c/a increased with increasing the excess Ba and saturated at $x = 0.02$. This can be interpreted in terms of the removal of Ba deficiency in BT(x) and A-site substitution in BNT. According to the Shannon's effective

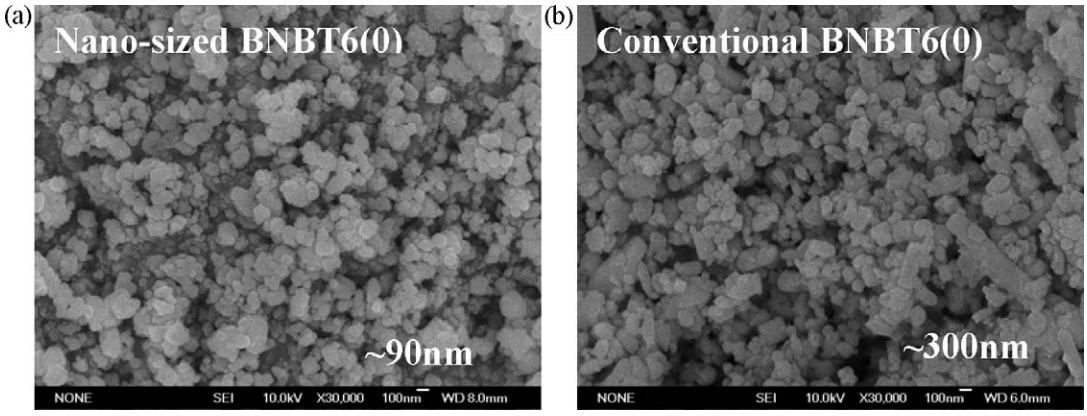

Fig. 6. SEM micrograph of the (a) high energy milled BNBT6(0) and (b) ball-milled BNBT6(0).

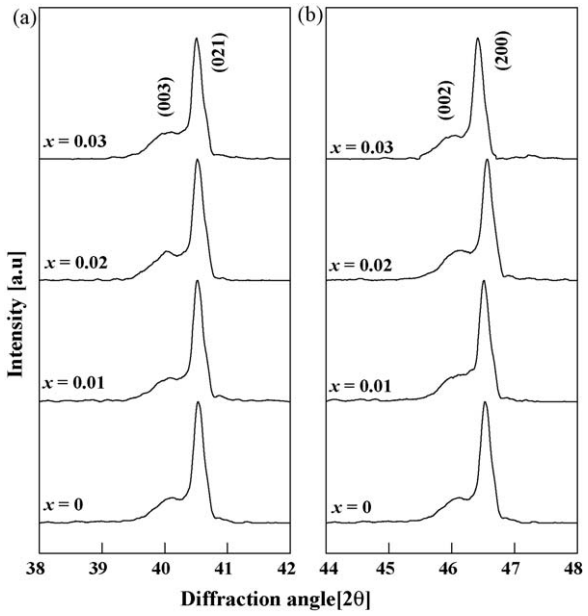

Fig. 8. X-ray diffraction patterns of the BNBT6(x) specimens with various amounts of excess Ba in the 2θ ranges of (a) 38–42° and (b) 44–48°.

radius [27], Na^+, Bi^{3+} and Ba^{2+} with a coordination number of twelve have radius of 1.39, 1.30 and 1.61 Å, respectively, while Ti^{4+} and Ba^{2+} with a coordination number of six possess radius of 0.61 and 1.35 Å, respectively. It can be speculated that excess Ba^{2+} cannot enter into the B-site of BT, but it can preferentially occupy the Ba deficiency site. This in turn increases the tetragonality of BT, which ultimately improved the tetragonality of BNBT6(x). Excess Ba enter into A-site vacancies of BT to fill up the Ba vacancies during the pre-synthesis of BT. After fulfilling the Ba deficiency, it is probable that Ba occupy A-site of BNT from consideration of ionic radius. Whereas, comparing the radius of Ba^{2+} with Bi^{3+} and Na^+, Ba^{2+} can enter into Na^+ site of BNT according to Hume–Rothery rules, but it is not easy to enter into Bi^{3+} site because the difference of radius between Ba and Bi ion site of BNT is greater than 15%. With relatively large size, the incorporation

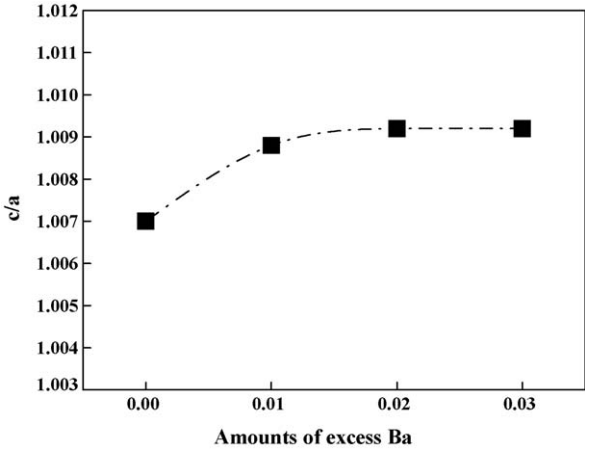

Fig. 9. Variations of lattice constant ratio (c/a) as a function of excess Ba amount.

of the excess Ba ion continuously increase the tetragonality of BNBT6(x) up to $x = 0.02$. On the other hand, the tetragonality of BNBT6(x) saturated at $x = 0.02$ and there is no further increase of tetragonality for the BNBT6(0.03) composition. It can be speculated that solubility of excess Ba ion within BNBT6(x) is 0.02 mol and it precipitates into secondary phase as the excess Ba ion increases to 0.03 mol. Thus, it can be considered that excess Ba ion fills up the Ba deficiency at first, then enters into Na^+ site and hence it is precipitated into secondary phase as increasing to 0.03 mol. As a consequence, there is no significant increase in the c/a ratio.

The micrographs of the sintered specimens of nano-sized BNBT6(x) are shown in Fig. 10(a)–(d). As can be seen Fig. 10 (a)–(d), grain shapes of the nano-sized BNBT6(x) are polyhedral and the average grain size of all samples appeared to be 1.6–1.8 μm. All of the nano-sized specimens showed high sintered density of ~5.94 g/cm^3, corresponding to the relative density of ~99%. Comparing the microstructure of nano-sized BNBT6(0) with that of conventional BNBT6(0), the grain shape of the conventional BNBT6(0) is squared rod shaped as shown in Fig. 10(a) and (e). Besides, conventional BNBT6(0) has a lower sintered density of 5.67 g/cm^3 than those of the nano-sized specimens as presented in Fig. 11. The observed equilibrium shape change of grains for nano-sized BNBT6(x) seems to be closely related with the increase of the sintered density. Considering the fact that pre-synthesized and nano-milled BNT6, BT(x) enhance reaction activity and increase the contact area, these processes may play a key role in achieving high density and fine grain size. To investigate the effects of manufacturing process and nano-sized powders, the piezoelectric and dielectric properties of two types BNBT6(0) samples sintered at same temperature are measured and listed in Table 2. The piezoelectric and dielectric properties of the nano-sized BNBT6(0) show higher values compared with those of the conventional BNBT6(0). The observed increase of piezoelectric and dielectric properties can be interpreted as the effects of the higher density and the coherency of grain boundary caused by equilibrium shape. Similarly, it was reported that in case of PZT the dielectric constant and piezoelectric properties increased with decreasing porosity [28]. It can be considered that the modified process increases the sintered density and decreases the porosity, and this in turn accompanies the increase of piezoelectric and dielectric properties.

3.3. Effects of the excess barium on the piezoelectric/dielectric properties and depolarization temperature

The piezoelectric and dielectric properties of BNBT6(x) specimens are shown in Fig. 12 (a) and (b). BNBT6(0.02) shows the maximum value of the planar electromechanical coupling factor (k_p) of 38%, the piezoelectric constant (d_{33}) of 198 pC/N. On the other hand, the relative dielectric permittivity (K^T_{33}) steadily increases with increasing the excess Ba content to 0.03 mol. However, the mechanical quality factor (Q_m) decreases with increasing excess Ba content and shows minimum value at the composition of BNBT6(0.02). The Q_m

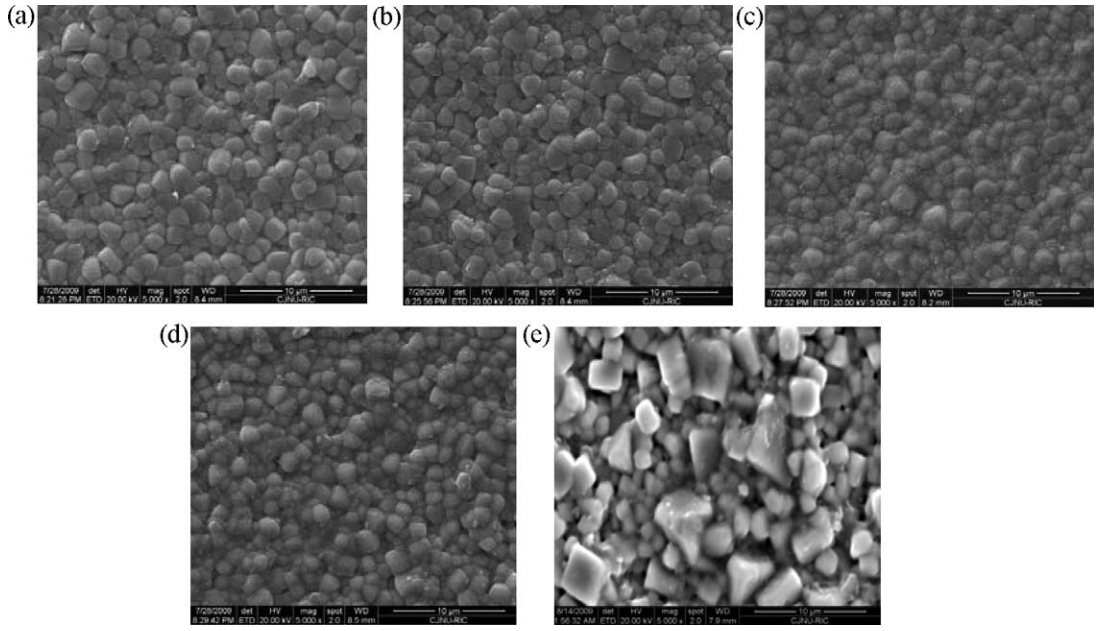

Fig. 10. SEM micrographs of the BNBT6(x) specimens with (a) $x = 0$, (b) $x = 0.01$, (c) $x = 0.02$, (d) $x = 0.03$ and (e) conventional BNBT6(0) sintered at 1140 °C for 2 h.

value then sharply increases to the maximum of 175 for the BNBT6(0.03) specimens. All of these phenomenon can be attributed to the effect of Ba. From the ICP results of BT(x), Ba/Ti mixing mole ratio of 1.00 corresponds to Ti-excess sample and Ba/Ti mixing mole ratio of 1.02 and 1.03 correspond to Ba excess samples, while Ba/Ti mixing mole ratio of 1.01 almost corresponds to equimolar sample. It was reported that in case of excess-Ti with a mixing ratio of 0.96, $Ba_2Ti_5O_{12}$ could be identified as a secondary phase, which is not a ferroelectric phase and it in turn decreases the dielectric and piezoelectric properties [29]. As in the reference, when excess Ba added up to 0.01 mol, Ba deficiency can be eliminated, leading to decrease in oxygen vacancy caused by Ba deficiency. And with further addition of Ba (0.02 mol), excess Ba can enter into A-site of BNT6. Considering the radius matching principle, it is highly probable that Ba^{2+} cannot enter into the B-site of BNBT6(x) perovskite, rather can occupy A-site. When excess Ba^{2+} enter into the Bi^{3+} site, the charge compensation will occur by the creation of oxygen vacancy, resulting in a decrease of the piezoelectric and dielectric properties [25]. Thus, the substitution of Bi^{3+} by Ba^{2+} cannot explain the increase in the piezoelectric and dielectric properties at BNBT6(0.02). When the Ba^{2+} occupy the Na^{+} site in a BNBT6(x) composition, Ba^{2+} acts as a donor leading to some A-site vacancies, which facilitates the motion of the domain wall so as to improve the piezoelectric and dielectric properties [25]. From the analysis above, rapid increase in k_p and d_{33} in BNBT6(0.02) can be explained by the easy domain wall motion due to some A-site vacancies created by Ba^{2+} addition. In addition to these, relatively higher sintered density and homogenous grain size also contribute to the improvement of piezoelectric properties. The piezoelectric properties rapidly decrease as excess Ba ion exceeds 0.02 mol. For Ba excess samples having a Ba/Ti ratio of 1.03, a secondary phase Ba_2TiO_4 may be formed and which can negatively influence the piezoelectric property [29]. On the other hand, the K^T_{33} rapidly increases as increasing the excess Ba amount to 0.03 mol. It can be explained that Ba deficiency caused by dissolution tends to result in an undesired secondary phase such as $Ba_2Ti_5O_{12}$ and this phase decrease the K^T_{33} in BNBT6(0). However, the K^T_{33} rapidly increase as excess Ba ions fill up the deficiency of BT, resulting in removal of

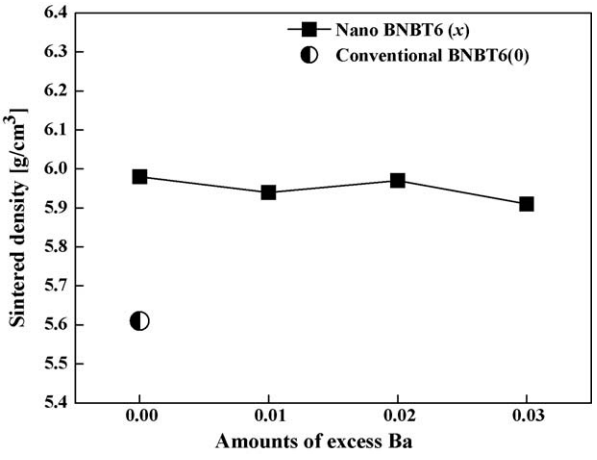

Fig. 11. Variations of sintered density as a function of excess Ba. The marked ◐ designates the sintered density of conventional BNBT6(0).

Table 2
The comparison characteristics of the ceramic specimens which were sintered at 1140 °C fabricated by two different processes.

Specimen	Density [g/cm^3]	d_{33} [pC/N]	K^T_{33}	k_p [%]	Q_m
Nano-sized BNBT6(0)	5.98	179	748	33.8	117
Conventional BNBT6(0)	5.67	131	714	21	125

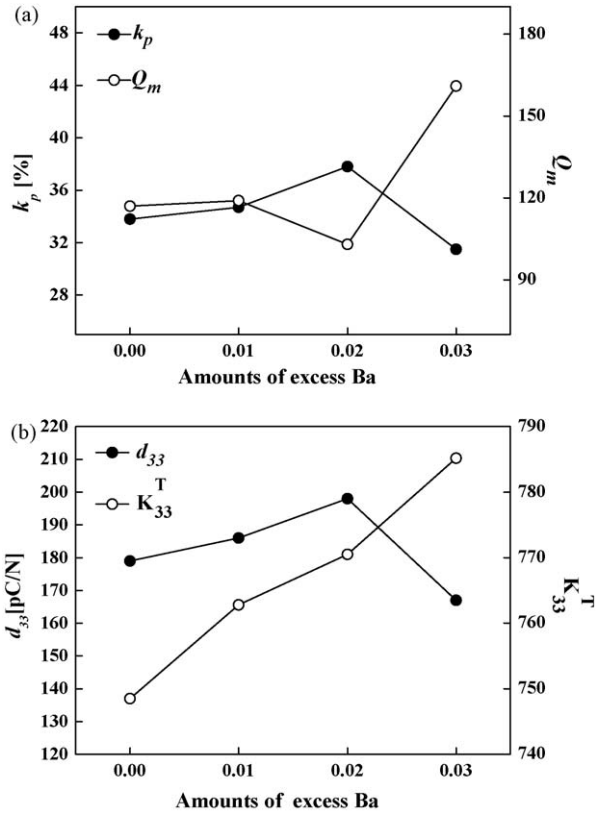

Fig. 12. Variations of piezoelectric and dielectric properties as a function of excess Ba amounts for nano-sized BNBT6(x): (a) planar electromechanical coupling factor (k_p) and mechanical quality factor (Q_m) and (b) piezoelectric constant (d_{33}) and relative dielectric permittivity (K^T_{33}).

detrimental $Ba_2Ti_5O_{12}$ pyrochlore phase. Furthermore, even if the excess Ba increases to 0.03 mol, the K^T_{33} increase to maximum value despite of the second phase, while piezoelectric property decreases. It has been reported that for BT having a Ba/Ti ratio of 1.03, formation of Ba_2TiO_4 phase increased the internal stress, which enhanced K^T_{33} to 1800 [29]. According to this report, since the Ba_2TiO_4 can exist in the BNBT6(0.03) composition, the K^T_{33} shows the maximum value as the same reason. However, the piezoelectric property decreases because of non-ferroelectric Ba_2TiO_4 phase. Besides, the variation of Q_m shows different behavior compared with othe piezoelectric properties. It is well known that the decrease of oxygen vacancy and increase of A-site vacancy increase the domain mobility, resulting in a decrease of Q_m. Hence, it decreases as increasing the excess Ba to 0.02 mol. However, the Q_m rapidly increases as increasing excess Ba to 0.03 mol. As previously mentioned, it can be interpreted as the increase of internal stress caused by the formation of Ba_2TiO_4. In general, the increase of the internal stress restricts the domain mobility and accompanies a significant increase of Q_m.

Fig. 13 shows the temperature dependence of the dielectric properties with various amounts of excess Ba. The dielectric behavior is rather analogous to those previously observed in BNBT ceramics with MPB compositions [30]. The inflection point designated T_d in Fig. 13 indicates the characteristic of phase transition. The T_d, corresponding to the ferroelectric–antiferroelectric transition, is termed as the 'depolarization temperature' [30]. On further heating, the specimens exhibit peak broadening near T_{max}, where T_{max} is the temperature of the peak dielectric permittivity. In this work, the coexistence of Bi^{3+}, Na^+ and Ba^{2+} at A-site could introduce a relaxor ferroelectric behavior, which was also proved by Saïd and co-workers [31,32]. As shown in Fig. 13, one can see that the depolarization temperature slightly decreases within a range of x = 0–0.01 mol [T_d = 96.7 °C for BNBT6(0) and T_d = 94.1 °C for BNBT6(0.01)], and then tends to rapidly decrease with excess Ba amounts of 0.02 mol [T_d = 89.1 °C for BNBT6(0.02)]. In addition to this, the T_d keeps unchanged

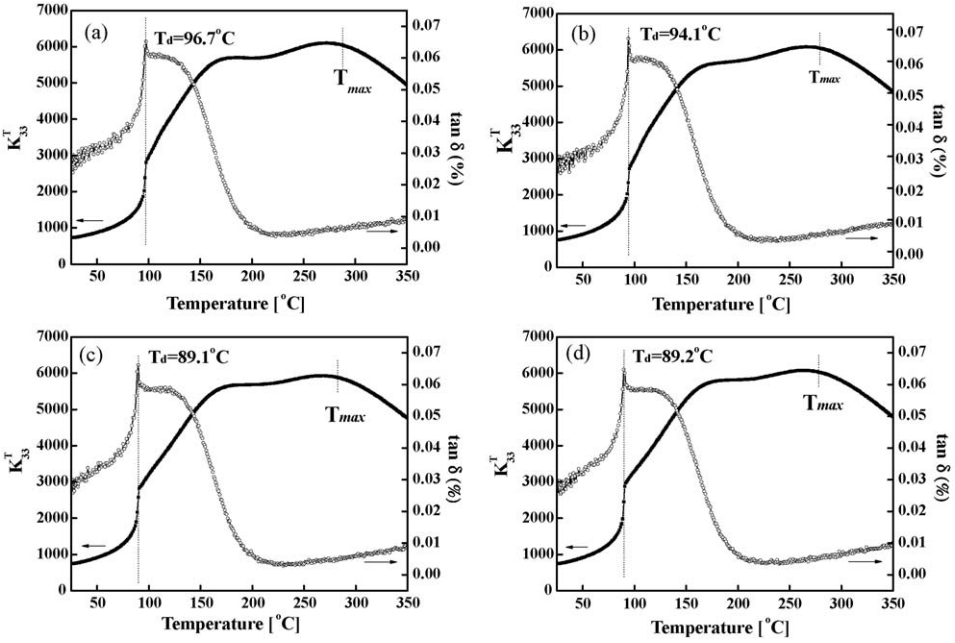

Fig. 13. Temperature dependence of dielectric properties of the BNBT6(x) specimens with various amounts of excess Ba: (a) x = 0, (b) x = 0.01, (c) x = 0.02, and (d) x = 0.03.

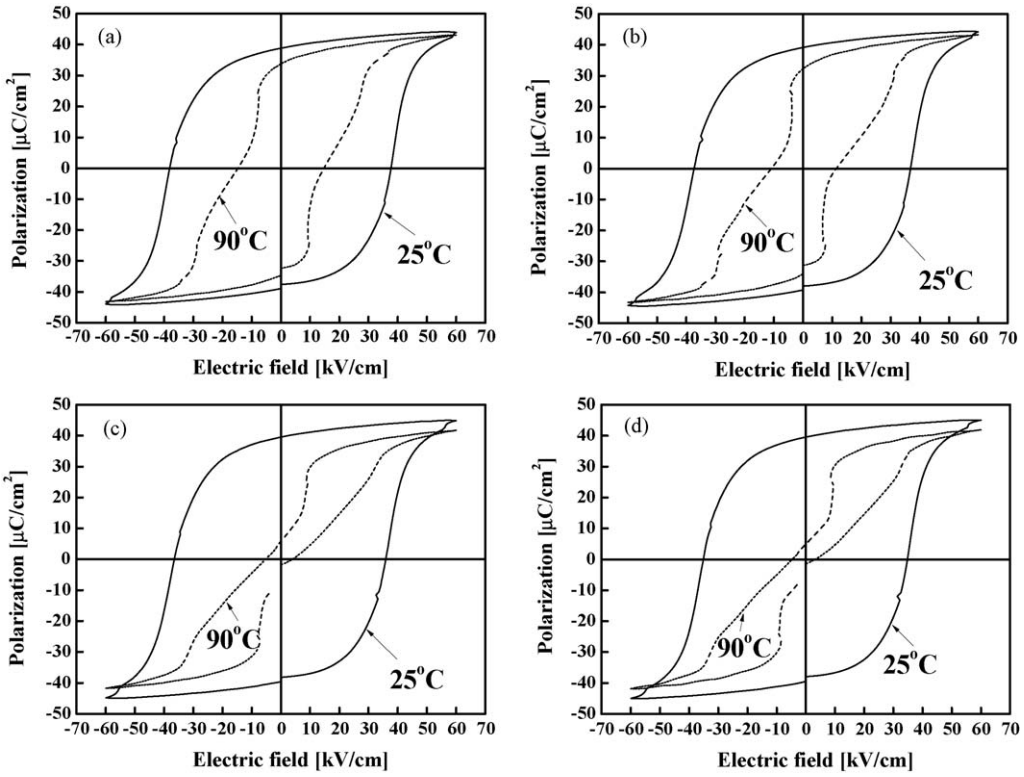

Fig. 14. *P–E* hysteresis loops measured at room temperature and around T_d temperature for the BNBT6(x) specimens with various amounts of excess Ba: (a) $x = 0$, (b) $x = 0.01$, (c) $x = 0.02$, and (d) $x = 0.03$.

with higher excess Ba of 0.03 mol [$T_d = 89.2\ ^\circ$C for BNBT6(0.03)]. The variation of the depolarization temperature with excess Ba amount reveals a decrease in the temperature stability of ferroelectric domains at relatively high excess Ba amounts. These phenomena can be comprehended with respect to the formation of A-site vacancies due to the incorporation of excess Ba into the structure. For [ABO_3]-type perovskite ferroelectrics, the stability of ferroelectric domains depends on the coupling between the ferroelectrically active [BO_6] octahedral via A-site cations [33]. The generation of A-site vacancies reduce the degree of the coupling between the [BO_6] octahedral and thereby reduce the stability of ferroelectric domains. Comparing BNBT6(0) with BNBT6(0.01) composition, the decrease of the T_d is smaller than that of BNBT6(0.02). This infers that the A-site vacancy effect on the stability of ferroelectric domains is minimal for these specimens, which can be explained by filling up the Ba deficiency as shown in Table 1. It is logical to deduce that the A-site vacancy effect would turn to be substantial at relatively higher excess Ba amounts. This may account for the remarkably decreased T_d (∼89.1 °C) for the specimen with excess Ba of 0.02 mol. In addition to this, further increase of excess Ba to 0.03 mol makes the T_d decrease to ∼89.2 °C, which value is similar to the specimens containing excess Ba of 0.02 mol. Further evidence for the depolarization temperature was obtained by examining the variation of polarization–electric field (*P–E*) hysteresis loop as shown in Fig. 14. At room temperature, typical ferroelectric *P–E* hysteresis loops were observed for these specimens. At this temperature, all specimens have a similar remnant polarization (P_r) value around 39.5 μC/cm^2. On the other hand, the hysteresis loops measured at 90 °C become narrower and show an antiferroelectric double-like hysteresis, reflecting the appearance of an antiferroelectric state. In addition to this, these data reveal that the double hysteresis loops still retain different degrees of remnant polarization (P_r). This can be ascribed to the coexistence of ferroelectric and antiferroelectric states in these specimens. The measuring temperature was chosen at 90 °C, which is lower than T_d of the BNBT6(0) and BNBT6(0.01) compositions and higher than T_d for the BNBT6(0.02) and BNBT6(0.03) compositions, the remnant polarization (P_r) and coercive field (E_c) for the former two specimens have a higher value than those of the latter two specimens. These results support that the decrease of depolarization temperature is closely related with A-site vacancy, suggesting a decrease in temperature stability of ferroelectric state at a relatively high excess Ba amount.

4. Conclusions

The effects of manufacturing process and the amount of excess Ba on the sintering temperature, microstructure and dielectric/piezoelectric properties have been analyzed systematically for BNBT ceramics of near MPB composition. The effect of pre-milled starting powders and separately synthesized BNT and BT on the reaction temperature and the crystal structure have been examined. It has revealed that the pre-milling process effectively lowered the reaction temperature for BNT and BT synthesis. A fully stabilized perovskite phase was observed in spite of the much lower reaction temperature for both BNT and $Ba_{(1+x)}TiO_3$. Separate preparation of fully

stabilized perovskite BNT and BT facilitates the BNT–BT solid solution formation without any further calcination step. Through microstructure observations, significant improvement of grain morphology, sintered density and piezoelectric/dielectric properties were found in nano-sized BNBT(0) compared to the conventional one. The variation of the piezoelectric and dielectric properties of the nano-sized BNBT6(x) could be interpreted on the basis of excess Ba. The highest value of d_{33} and k_p were found for Ba excess of 0.02 mol, which has been interpreted as the easy domain wall motion due to some A-site vacancies created by Ba^{2+} addition. The variation of T_d with excess Ba revealed a decrease in the temperature stability of ferroelectric domains at relatively high excess Ba amounts. P–E hysteresis results also supported that the decrease of depolarization temperature was closely related with A-site vacancy.

Acknowledgements

This research was supported by the Regional Innovation Center (RIC) Program which was conducted by the Ministry of Commerce, Industry and Energy of the Korean Government and by a grant from the Academic Research Program of Chungju National University in 2009.

References

[1] G.M. Lee, Agency for technology and standards industry and energy of the Korean Government, in: Seminar on EU Product-Related Regulations, 2004, p. 6.
[2] H. Nagata, T. Takenaka, Additive effects on electrical properties of $(Bi_{1/2}Na_{1/2})TiO_3$ ferroelectric ceramics, J. Eur. Ceram. Soc. 21 (2001) 1299–1302.
[3] G.A. Smolenskii, V.A. Isupov, A.I. Agranovskaya, N.N. Krainik, New ferroelectrics of complex compositon, Sov. Phys. Solid State 2 (1961) 2651–2654.
[4] K. Sakata, Y. Masuda, Ferroelectric and antiferroelectric properties of $(Na_{0.5}Bi_{0.5})TiO_3$–$SrTiO_3$ solid solution ceramics, Ferroelectrics 7 (1) (1974) 347–349.
[5] T. Takenaka, K. Sakata, K. Toda, Piezoelectric properties of $(Bi_{1/2}Na_{1/2})TiO_3$-based ceramics, Ferroelectrics 106 (1) (1990) 375–380.
[6] T. Takenaka, K. Maruyama, K. Sakata, $(Bi_{1/2}Na_{1/2})TiO_3$–$BaTiO_3$ system for lead-free piezoelectric ceramics, Jpn. J. Appl. Phys. 30 (1991) 2236–2239.
[7] N. Ichinose, K. Udagawa, Piezoelectric properties of $(Bi_{1/2}Na_{1/2})TiO_3$-based ceramics, Ferroelectrics 169 (1995) 317–325.
[8] T. Takenaka, T. Okuda, K. Takegahara, Lead-free piezoelectric ceramics based on $(Bi_{1/2}Na_{1/2})TiO_3$–$NaNbO_3$, Ferroelectrics 196 (1) (1997) 175–178.
[9] A. Sasaki, T. Chiba, Y. Mamiya, E. Otsuki, Dielectric and piezoelectric properties of $(Bi_{0.5}Na_{0.5})TiO_3$–$(Bi_{0.5}K_{0.5})TiO_3$ systems, Jpn. J. Appl. Phys. 38 (1999) 5564–5567.
[10] Y. Wu, H. Zhang, Y. Zhang, J. Ma, D. Xie, Lead-free piezoelectric ceramics with composition of $(0.97–x)Na_{1/2}Bi_{1/2}TiO_3$–$0.03NaNbO_3$–$x$Ba-$TiO_3$, J. Mater. Sci. 38 (5) (2003) 987–994.
[11] H. Nagata, M. Yoshida, Y. Makiuchi, T. Takenaka, Large piezoelectric constant and high curie temperature of lead-free piezoelectric ceramic ternary system based on bismuth sodium titanate–bismuth potassiumtitanate–barium titanate near the morphotropic phase boundary, Jpn. J. Appl. Phys. 42 (2003) 7401–7403.
[12] L. Wu, D.Q. Xiao, D.M. Lin, J.G. Zhu, P. Yu, Synthesis and properties of $[Bi_{0.5}(Na_{1-x}Ag_x)_{0.5}]_{1-y}Ba_yTiO_3$ piezoelectric ceramics, Jpn. J. Appl. Phys. 44 (2005) 8515–8518.
[13] A. Herabut, A. Safari, Processing and electromechanical properties of $(Bi_{0.5}Na_{0.5})_{(1-1.5x)}La_xTiO_3$ ceramics, J. Am. Ceram. Soc. 80 (11) (1997) 2954–2958.
[14] H.D. Li, C.D. Feng, P.H. Xiang, Electrical properties of La^{3+}-doped $(Na_{0.5}Bi_{0.5})_{0.94}Ba_{0.06}TiO_3$ ceramics, Jpn. J. Appl. Phys. Part I 42 (12) (2003) 7387–7391.
[15] H.D. Li, C.D. Feng, W.L. Yao, Some effects of different additives on dielectric and piezoelectric properties of $(Bi_{1/2}Na_{1/2})TiO_3$–$BaTiO_3$ morphotropic-phase-boundary composition, Mater. Lett. 58 (7–8) (2004) 1194–1198.
[16] X. Zhou, H.S. Gu, Y. Wang, W.Y. Li, T.S. Zhou, Piezoelectric properties of Mn-doped $(Na_{0.5}Bi_{0.5})_{0.92}Ba_{0.08}TiO_3$ ceramics, Mater. Lett. 59 (13) (2005) 1649–1652.
[17] T. Takenaka, Piezoelectric properties of some lead-free ferroelectric ceramics, Ferroelectrics 230 (1) (1999) 87–98.
[18] M. Raghavender, G.S. Kumar, G. Prasad, Modification of dielectric relaxations in sodium bismuth titanate with samarium doping, J. Phys. Chem. Solids 67 (2006) 1803–1808.
[19] H. Nagata, T. Shinya, Y. Hiruma, T. Takenaka, I. Sakguchi, H. Haneda, Piezoelectric properties of bismuth sodium titanate ceramics, Ceram. Trans. 167 (2005) 213–221.
[20] T. Takenaka, H. Nagata, Current status and prospects of lead-free piezoelectric ceramics, J. Eur. Ceram. Soc. 25 (12) (2005) 2693–2700.
[21] IRE Standards on Piezoelectric Crystals: Measurements of Piezoelectric Ceramics, in: Proceedings of the Institute of Radio Engineers, vol. 49, no. 7, 1961, pp. 1161–1169.
[22] M. Vieth, S. Mathur, N. Lecerf, V. Huch, T. Decker, H.P. Beck, W. Eiser, R. Haberkom, Sol-gel synthesis of nano-scaled $BaTiO_3$, $BaZrO_3$ and $BaTi_{0.5}Zr_{0.5}O_3$ oxides via single-source alkoxide precursors and semi-alkoxide routes, J. Sol.–Gel. Sci. Technol. 17 (2) (2000) 145–158.
[23] A. Beauger, J. Mutin, J. Niepce, Synthesis reaction of metatitanate $BaTiO_3$, J. Mater. Sci. 18 (10) (1983) 3041–3046.
[24] D.H. Yoon, Tetragonality of barium titanate powder for a ceramic capacitor application, J. Ceram. Process. Res. 7 (4) (2006) 343–354.
[25] B.J. Chu, D.R. Chen, G.R. Li, Q.R. Yin, Electrical properties of $Na_{1/2}Bi_{1/2}TiO_3$–$BaTiO_3$ ceramics, J. Eur. Ceram. Soc. 22 (2002) 2115–2121.
[26] M. Chen, Q. Xu, B.H. Kim, B.K. Ahn, J.H. Ko, W.J. Kang, O.J. Nam, Structure and electrical properties of $(Na_{0.5}Bi_{0.5})_{1-x}Ba_xTiO_3$ piezoelectric ceramics, J. Eur. Ceram. Soc. 28 (2008) 843–849.
[27] R.D. Shannon, Revised effective ionic radii and systematic studies of interatomic distances in halides and chalcogenides, Acta Cryst. A32 (1976) 751–767.
[28] G.H. Haertling, W.J. Zimmer, Analysis of hot pressing parameters for lead–zirconate–lead titanate ceramics containing two atom percent bismuth, Am. Ceram. Soc. Bull. 45 (1966) 1084–1089.
[29] S.B. Deshpande, H.S. Potdar, M.M. Patil, V.V. Deshpande, Y.B. Khollam, Dielectric properties of $BaTiO_3$ ceramics prepared from powders with bimodal distribution, J. Ind. Eng. Chem. 12 (4) (2006) 584–588.
[30] M.S. Yoon, Y.G. Lee, S.C. Ur, Effects of co-doped CaO/MnO on the piezoelectric/dielectric properties and phase transition of lead-free $(Bi_{0.5}Na_{0.5})_{0.94}Ba_{0.06}TiO_3$ piezoelectric ceramics, J. Electroceram. 23 (2009) 564–571.
[31] S. Saïd, J.P. Mercurio, Relaxor behavior of low lead and lead free ferroelectric ceramics of the $Na_{0.5}Bi_{0.5}TiO_3$–$PbTiO_3$ and $Na_{0.5}Bi_{0.5}$-TiO_3–$K_{0.5}Bi_{0.5}TiO_3$ systems, J. Eur. Ceram. Soc. 21 (2001) 1333–1336.
[32] J.R. Gomah-Pettry, S. Saïd, P. Marchet, J.P. Mercurio, Sodium–bismuth titanate based lead-free ferroelectric materials, J. Eur. Ceram. Soc. 24 (6) (2004) 1165–1169.
[33] X. Dai, A. DiGiovanni, D. Viehland, Dielectric properties of tetragonal lanthanum modified lead zirconate titanate ceramics, J. Appl. Phys. 74 (5) (1993) 3399–3405.